Eur Radiol (2015) 25:940–949
DOI 10.1007/s00330-014-3493-2

GASTROINTESTINAL

Mucinous cystic neoplasms and serous cystadenomas arising in the body-tail of the pancreas: MR imaging characterization

Riccardo Manfredi · Anna Ventriglia · William Mantovani · Sara Mehrabi · Enrico Boninsegna · Giuseppe Zamboni · Roberto Salvia · Roberto Pozzi Mucelli

Received: 26 March 2014 / Revised: 10 October 2014 / Accepted: 10 November 2014 / Published online: 23 November 2014
© European Society of Radiology 2014

Abstract
Purpose To identify magnetic resonance (MR)/MR cholangiopancreatography (MRCP) imaging signs helpful in the differential diagnosis between serous cystadenomas (SCAs) and mucinous cystic neoplasms (MCNs), arising from the body/tail of the pancreas.
Material and methods This retrospective study had institutional review board approval and informed consent was waived. Fifty-three patients with non-communicating cystic pancreatic neoplasm of the body/tail, undergoing MR/MRCP, were included. Qualitative image analysis assessed the macroscopic pattern, number of cysts, presence of central scar, contrast enhancement of peripheral wall, and mural nodules. Quantitative analysis assessed the maximum diameter of the neoplasm, thickness of the peripheral wall, and calibre of the upstream main pancreatic duct.
Results Histopathology results revealed that 27/53 (51 %) were SCAs, 26/53 (49 %) were MCNs. Microcystic pattern was observed in 88.2 % of SCAs and 11.8 % of MCNs; macrocystic pattern was observed in 90.5 % of MCNs and 9.5 % of SCAs ($p<0.0001$). Central scar was detected in 29.6 % of SCAs and no MCNs ($p=0.003$). Contrast enhancement of the peripheral wall was evident in 99.5 % of MCNs and 11.5 % of SCAs ($p<0.0001$); mural nodules were depicted in 94.1 % of MCNs and 5.9 % of SCAs ($p<0.0001$). Median maximum diameter was 54 mm for MCNs, 32 mm for SCAs ($p=0.001$); median wall thickness was 4 mm for MCNs, 2 mm for SCAs ($p<0.0001$).
Conclusions Macrocystic pattern, enhancement of a peripheral wall and mural nodules are suggestive of MCNs; whereas microcystic pattern, lack of peripheral wall and central scar are suggestive of SCAs.
Key Points
- *MCNs have macrocystic patterns, contrast enhancement of the peripheral wall and mural nodules*
- *Microcystic pattern and central scar are suggestive of SCA*
- *Mural nodules detected in MCNs correlate with epithelial dysplasia*
- *Chronic obstructive pancreatitis is equally depicted in patients with MCNs and SCAs*

Keywords Pancreas, cystic neoplasm · Pancreas, MR · Pancreatic ducts · Main pancreatic duct, MR · Obstructive chronic pancreatitis, MR

R. Manfredi (✉) · A. Ventriglia · S. Mehrabi · E. Boninsegna · R. Pozzi Mucelli
Department of Radiology, University of Verona, P.le L.A. Scuro 10, 37134 Verona, Italy
e-mail: riccardo.manfredi@univr.it

W. Mantovani
Department of Public Health and Prevention, Provincial Health Services, A. Degasperi 79, 38123 Trento, Italy

G. Zamboni
Department of Pathology, University of Verona, P.le L.A. Scuro 10, 37134 Verona, Italy

R. Salvia
Department of Surgery, University of Verona, P.le L.A. Scuro 10, 37134 Verona, Italy

Introduction

Cystic neoplasms occurring in the pancreas are frequently asymptomatic and incidentally discovered by means of diagnostic imaging [1–5]. These neoplasms show a different biological behaviour and treatment; therefore lesion characterization represents a medical need in patient management. In this settings, non-operative histological diagnosis is inaccurate in approximately 25 % of the cases [6], and because of this limitation, diagnostic imaging plays a major role in this task.

Mucinous cystic neoplasms (MCNs) of the pancreas are presumably de novo cystic tumours observed almost exclusively in women (male to female ratio < 1:20), arising in 93–97 % of the cases in the body/tail of the gland and typically defined by the lack of communication with the pancreatic ductal system [1–5].

The histological hallmark of MCNs is a dense cellular ovarian-type stroma which produces mucin. Stromal cells are positive for progesterone and oestrogen receptors, suggesting a derivation from the ovarian primordium [1, 3–6].

Biologically, the mucin-producing epithelium of MCN exhibits features of an adenoma–carcinoma sequence; therefore MCNs should be considered neoplasms with overt or latent malignancy and candidates for surgical resection [3, 7, 8].

Pancreatic resection, however, is associated with substantial risk of morbidity and measurable mortality [9]. Therefore a preoperative lesion characterization is necessary, since other non-communicating cystic pancreatic neoplasms, such as serous cystadenomas (SCAs), show a benign biological course with no indication for surgery, but clinical-radiological follow-up [10, 11].

The differential diagnosis between MCNs and IPMNs relies on the demonstration of the presence/absence of communication with the pancreatic duct system [12–15]. More challenging is the differential diagnosis between non-communicating cystic neoplasms, such as MCN and SCA, arising in the body/tail of the pancreas, where MCN is almost exclusively located [11]. However, this differential represents a medical need in clinical practice. The same problem does not occur for cystic tumours located in the head of the pancreas, since MCNs do not occur in this site.

Magnetic resonance (MR) imaging is potentially able to cover this medical need, because of its intrinsic high soft tissue contrast resolution [16, 17], being able to depict internal features of pancreatic cystic neoplasms, such as septa and cysts contents, and by exploiting the lesion-ductal system relationship [18], by means of MR/MR cholangiopancreatography (MRCP) imaging.

The aim of our study is to identify signs on MR/MRCP imaging helpful in the differential diagnosis between SCAs and MCNs, arising from the body/tail of the pancreas.

Material and methods

Patient population

Our retrospective study was approved by the institutional review board (IRB) and informed consent was waived. A search of our institution's radiology, pathology and medical records, between January 2008 and December 2011, identified 169 patients with cystic neoplasms of the pancreas, who were considered for inclusion in our study.

Patients were recruited in our study according to the following inclusion criteria: cystic neoplasm arising in the body/tail of the pancreas (left to the superior mesenteric vein), histological confirmation by means of either surgical procedure or biopsy (surgical, endoscopic, percutaneous) and preoperative MRI/MRCP examination. Exclusion criteria included lack of available preoperative MR imaging performed at our institution (38 patients), cystic lesions communicating with the pancreatic duct system (73 patients) and cystic lesions with a histological diagnosis different from SCA and MCA (5 patients).

Thus, the study population encompassed 53 patients, with a mean age of 50.7 years (range 16–79.3 years), consisting of 42 women (mean age 48.8 years; range 16–79.3 years) and 11 men (mean age 57.8 years; range 36.1–78.8 years).

Clinical findings and laboratory data at diagnosis are reported in Table 1. All patients underwent MR imaging with MRCP, and biopsy or surgical procedure (Table 1). The mean time interval between MR imaging/MRCP and biopsy/surgery was 70.5 days (range, 1 day–7 months) (Table 1).

Magnetic resonance imaging

MR imaging was performed on a 1.5-T system (Magnetom Symphony, Siemens, Erlangen, Germany), using of a 4-channel phased array coil.

The patients were asked to fast 4–6 h before the examination. Furthermore, to eliminate overlapping fluid-containing

Table 1 Cystic neoplasms arising in the body/tail of the pancreas: patient population, clinical presentation, laboratory data and surgical procedures

		Patients (n=53)
Symptoms	Asymptomatic	36/53 (68 %)
	Abdominal pain	11/53 (21 %)
	Mild acute pancreatitis	5/53 (9 %)
	Diabetes	1/53 (2 %)
	Increased Tumour markers	5/53 (9 %)
Surgical procedure		37/53 (70 %) (Histopathology: 26/37 MCNs; 11/37 SCAs)
	Spleno-pancreatectomy	28
	Total pancreatectomy	5
	Middle pancreatectomy	2
	Gastro-jejunostomy	1
Biopsy		16/53 (30 %) (Histopathology: 16/16 SCAs)

MCNs mucinous cystic neoplasms, *SCAs* serous cystadenomas

organs on T2-weighted images, a negative contrast agent was administered before MR imaging. This consisted of 50–150 ml of superparamagnetic iron oxide particles (ferumoxsil, Lumirem, Guerbet, Aulnay-sous-Bois, France) 5–15 min before the beginning of the examination. No antiperistaltic drug was administered.

The MR imaging protocol is illustrated in Table 2, and specifically included:

- Chemical shift T1-weighted gradient echo axial images, with TE both in-phase and out-of-phase; axial fat-saturated T2-weighted rapid acquisition with relaxation enhancement (RARE) images; coronal and axial T2-weighted half Fourier RARE (HASTE, half Fourier single-shot turbo spin-echo) images; and axial fat-saturated T1-weighted gradient echo images.
- Sagittal and coronal oblique HASTE acquisitions with appropriate angulation (from 3–10, mean 6) were obtained to better visualize the whole pancreatic ductal system, as well as the biliary tree, both papillae, and the duodenum.
- Once the most appropriate plane to visualize the biliopancreatic duct system was identified, MRCP was performed in all patients using a two-dimensional half Fourier RARE (HASTE) heavily T2-weighted pulse sequence, during breath-hold.
- Dynamic study during injection of gadolinium chelates was obtained by means of a 3D volumetric gradient echo pulse sequence (VIBE, volumetric interpolated breath-hold examination) with fat saturation, along the axial plane, using parallel imaging (GRAPPA acceleration factor 2). A quadriphasic dynamic study was performed during 0.1 mmol/kg body weight gadolinium chelates injection (MultiHance, Bracco, Milan, Italy; Dotarem, Guerbet, Aulnay-sous-Bois, France) by means of a power injector (Medrad, Pittsburgh, Pennsylvania, USA) at 2–2.5 ml/s, by acquiring the pre-contrast phase, late arterial/pancreatic phase (35–45 s), portal venous phase (75–80 s) and delayed phase (>180 s).

Image analysis

MR/MRCP images were independently analysed by two radiologists experienced in gastrointestinal radiology (15 and 28 years, respectively) who were aware of the diagnosis of cystic lesion arising in the body/tail of the pancreas, but unaware of the histological diagnosis (serous cystadenoma vs. mucinous cystic neoplasm). Subsequently, image interpretation discrepancies were resolved by consensus, which was required in 35/742 (5 %) parameters analysed. The image analysis was performed on a workstation. In order to improve the objectivity of the data, quantitative image analysis was performed by a third radiologist (with 4 years of experience) not involved in the qualitative image analysis and unaware of the histological diagnosis, on a workstation using an electronic caliper.

Qualitative image analysis included the following parameters: macroscopic pattern of the cystic lesion using a size threshold of 2 cm (microcystic, <2 cm/macrocystic, ≥2 cm/mixed); number of cysts (unicystic/oligocystic, ≤5/multicystic, ≥6); lesion margins (sharp/irregular); signal intensity on T1-WI and T2-WI (hypointense/isointense/hyperintense relative to liver parenchyma); central scar (present/absent); contrast enhancement of intralesional septae, of the peripheral wall and of mural nodules as depicted on the portal venous/equilibrium phase of the dynamic study during gadolinium chelates administration; pattern of the upstream main pancreatic duct (MPD) (linear/tortuous); endoluminal filling defects in the MPD (present/absent); dilated side branches in the upstream pancreas (present/absent); hypointensity on T1-WI of the upstream pancreatic parenchyma (present/absent).

Table 2 Magnetic resonance (MR) imaging protocol: pulse sequences and parameters

Pulse sequence	Plane	TR (ms)	TE (ms)	Slice thickness (mm)	Parallel imaging
Chemical shift T1-weighted gradient echo	Axial	107–160	2.4–4.8	7–8	
Fat-saturated T2-weighted (RARE)	Axial	4,000–4,950	91–102	7–8	
T2-weighted half Fourier RARE (HASTE)	Coronal and axial	∞	60–102	4–6	
T1-weighted fat-saturated gradient echo	Axial	160–180	4	4–6	
T2-weighted half Fourier RARE (HASTE)	Sagittal and coronal oblique	∞	102–400	40–60	
2D half Fourier RARE (HASTE) MRCP	Coronal oblique	∞	1,100	40–80	
Fat-saturated 3D volumetric gradient echo (VIBE)	Axial	4.66	1.87	2.6–3	GRAPPA acceleration factor 2

TR repetition time, *TE* echo time, *RARE* rapid acquisition with relaxation enhancement, *HASTE* half Fourier single-shot turbo spin-echo, *MRCP* magnetic resonance cholangiopancreatography, *VIBE* volumetric interpolated breath-hold examination, *2D* two dimensional, *3D* three dimensional, *GRAPPA* generalized autocalibrating partially parallel acquisition, *ms* milliseconds

Quantitative image analysis included the following parameters: maximum diameter of the cystic neoplasm; thickness of peripheral wall (thickest segment, avoiding mural nodules); calibre of the upstream MPD (upstream of the cystic neoplasm); MPD was considered dilated when calibre measured at least 3 mm in the body and at least 2 mm in the tail.

Statistical analysis

The strength of the interobserver variability for the qualitative image analysis was assessed using *k* statistics as follows: less than 0.20, poor; 0.21–0.40, fair; 0.41–0.60, moderate; 0.61–0.80, good; 0.81–1.0, excellent agreement.

For the quantitative analysis, the distribution of continuous variables is reported as median and range. Categorical variables are presented as numbers and percentages. To assess post-treatment changes, McNemar's test was applied for categorical variables; whereas the paired sample *t* test (or the Wilcoxon test, in the case of a skewed distribution) was applied for continuous variables. When data were not normally distributed, we considered the *p* values obtained from non-parametric tests.

These analyses were performed by using SPSS software (SPSS for Windows, version 16.0; SPSS Chicago, IL, USA); *p* values were considered significant when no greater than 0.05.

Results

Histopathological analysis revealed that 27/53 (51 %) patients had a diagnosis of SCA, whereas 26/53 (49 %) patients had a diagnosis of MCN; among the MCNs, 21/26 (81 %) were adenomas and 5/26 (19 %) were carcinomas. MCNs were divided into non-invasive (n=25) and invasive neoplasms (n=1), using World Health Organization (WHO) guidelines [4]. Non-invasive MCNs were graded on the basis of the greatest degree of dysplasia into low-grade dysplasia (n=22), moderate dysplasia (n=2) and high-grade dysplasia (n=0).

Qualitative image analysis revealed that overall cystic neoplasms of the body/tail of the pancreas showed a macrocystic pattern in 21/53 (40 %) patients, microcystic pattern in 17/53 (32 %) and a mixed pattern in 15/53 (28 %) patients (Fig. 1). The interobserver variability was k=0.843.

The number of cysts observed within the cystic neoplasms showed an oligocystic (≤5 cysts) pattern in 24/53 (45 %) patients, a multicystic pattern (≥6 cysts) in 15/53 (28 %) patients and a unicystic pattern in 14/53 (26 %) patients (Fig. 2). The interobserver variability was k=0.671.

Lesion margins were sharp in 50/53 lesions (94 %) and irregular in 3/53 (6 %) (k=0.649).

On T1-WI cystic neoplasms of the body/tail of the pancreas appeared hypointense in 42/53 (79 %) patients, isointense in 6/53 (11 %) and hyperintense in 5/53 (9 %). The interobserver variability was k=0.681.

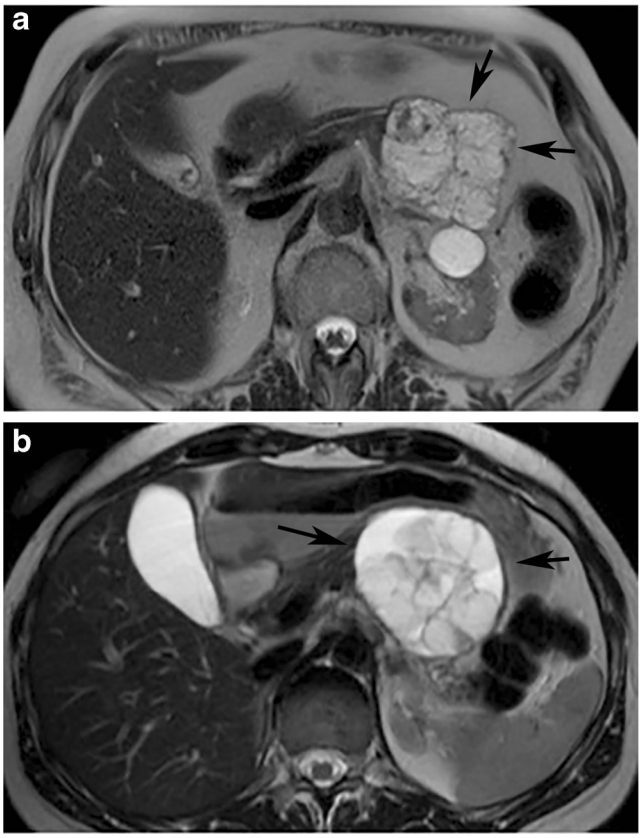


Fig. 1 Macroscopic pattern of cystic neoplasms arising in the body/tail of the pancreas: size of the cysts. **a** Axial T2-weighted half Fourier single-shot turbo spin-echo (HASTE) (TR/TE ∞/90 ms) image shows a cystic neoplasm of the body/tail of the pancreas with microcystic pattern (<2 cm) (*arrows*), which was a serous cystadenoma at histopathology. Microcystic pattern was observed in 88.2 % of serous cystadenomas (SCAs) and 11.8 % of mucinous cystic neoplasms (MCNs) (p<0.0001). **b** Axial T2-weighted turbo spin echo (TSE) (TR/TE 4,200/102 ms) image shows a cystic neoplasm of the body/tail of the pancreas with macrocystic pattern (≥2 cm) (*arrows*), which was an MCN at histopathology. Macrocystic pattern was observed in 90.5 % of MCNs and 9.5 % of SCAs (p<0.0001)

On T2-WI, cystic neoplasms appeared hyperintense in all 53/53 patients (k=1.000) (Figs. 1 and 2).

A central scar was depicted in 8/53 patients whereas was absent in 45/53 (85 %) patients (k=1.000) (Fig. 3).

Contrast enhancement of intralesional septae, during the portal venous phase of the dynamic study, was observed in 25/53 (47 %) of the patients; whereas a lack of enhancement was observed in 28/53 (53 %) of the patients (k=0.962).

Contrast enhancement of a peripheral wall was observed in 26/53 (49 %) patients, whereas it was absent in 27/53 (51 %) patients (k=0.962) (Fig. 4).

Contrast enhancement of mural nodules during the portal venous phase of the dynamic study was observed in 17/53 (32 %) patients whereas 36/53 (68 %) patients did not show mural nodules (k=0.774) (Fig. 5).

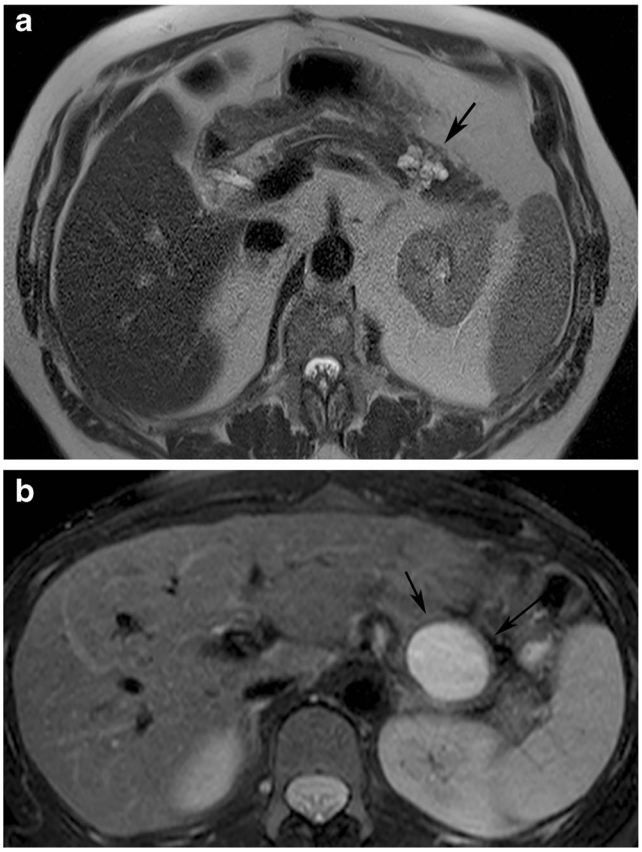


Fig. 2 Macroscopic pattern of cystic neoplasms arising in the body/tail of the pancreas: number of cysts. **a** Axial T2-weighted half Fourier single-shot turbo spin-echo (HASTE) (TR/TE ∞/90 ms) image shows cystic neoplasms of the body/tail of the pancreas with multicystic (≥6), microcystic pattern (*arrow*). Multicystic pattern was observed in 73.3 % of the cases of SCA and 26.7 % of the cases of MCN (p=0.054). **b** Axial T2-weighted fat-suppressed turbo spin echo (TSE) (TR/TE 4,200/90 ms) image shows a cystic neoplasm of the body/tail of the pancreas with unicystic, macrocystic pattern (*arrows*), which was an MCN at histopathology. Unicystic pattern was observed in 71.4 % of MCNs and 28.6 % of SCAs (p=0.054)

The upstream main pancreatic duct (MPD) appeared non-dilated with a linear path in 39/53 (74 %) patients, and dilated with a tortuous path in 14/53 (26 %) patients (k=0.564) (Fig. 6). Filling defects within the lumen of the MPD were observed in 3/53 (6 %) patients (k=0.548) and dilated side branches in the upstream pancreas in 7/53 (13 %) patients (k=0.547).

On T1-WI, the upstream pancreatic parenchyma appeared hyperintense in 48/53 (91 %) patients as did the downstream pancreas; whereas in 5/53 (9 %) patients it appeared hypointense (k=0.442).

Mucinous cystic neoplasms (MCNs; n=26)

MCNs showed a macrocystic pattern (≥2 cm) in 19/26 (73 %) of MCNs arising in the body/tail of the pancreas, mixed in 5/26 (19 %) and microcystic in 2/26 (8 %) (Figs. 1 and 2).

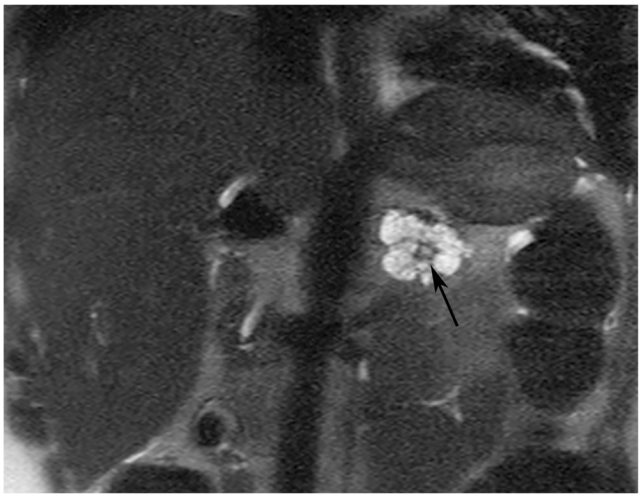


Fig. 3 Cystic neoplasms arising in the body/tail of the pancreas: central scar. Coronal fat-suppressed T2-weighted half Fourier single-shot turbo spin-echo (HASTE) (TR/TE ∞/90 ms) image shows a multicystic, microcystic cystic neoplasm of the body/tail of the pancreas with a central scar (*arrow*). A central scar was observed in 29.6 % of SCAs and none of the MCNs (p=0.003)

MCNs showed an oligocystic pattern (≤5 cysts) in 12/26 (46 %), unicystic pattern in 10/26 (38 %) and multicystic (≥6) in 4/26 (15 %) (Figs. 1 and 2).

Sharp margins were observed in 23/26 (88 %) of MCNs and irregular margins in 3/26 (12 %).

On T1-WI, MCNs appeared hypointense in 19/26 (73 %) of the cases, hyperintense in 4/26 (15 %) and isointense in 3/26 (12 %). On T2-WI, 26/26 MCNs arising in the body/tail of the pancreas appeared hyperintense (Figs. 1 and 2).

A central scar was observed in none of the MCNs.

Contrast enhancement of internal septae was observed in 10/26 (38 %) MCNs, whereas the contrast enhancement of the peripheral wall and of mural nodules were present respectively in 23/26 (88 %) and 16/26 (62 %) MCNs (Figs. 4 and 5). Mural nodules occurred in 14/16 non-invasive MCNs with low-grade dysplasia, 1/16 in non-invasive MCN with moderate dysplasia and in 1/16 invasive MCN.

The upstream MPD appeared dilated with a tortuous path in 5/26 (19 %) MCNs, whereas in 21/26 (81 %) the upstream MPD appeared non-dilated with a linear path (Fig. 6). Endoluminal filling defects within the lumen of the upstream MPD were observed in 2/26 (8 %) MCNs, and dilated side branches in the upstream pancreatic duct system were observed in 3/26 (12 %) of MCNs.

Hypointensity of the upstream pancreatic parenchyma was observed in 5/26 (19 %) of the MCNs arising in the body/tail of the pancreas.

Serous cystadenomas (SCAs; n=27)

SCAs showed a microcystic pattern in 15/27 (56 %) cases, a mixed pattern in 10/27 (37 %) and a macrocystic pattern in

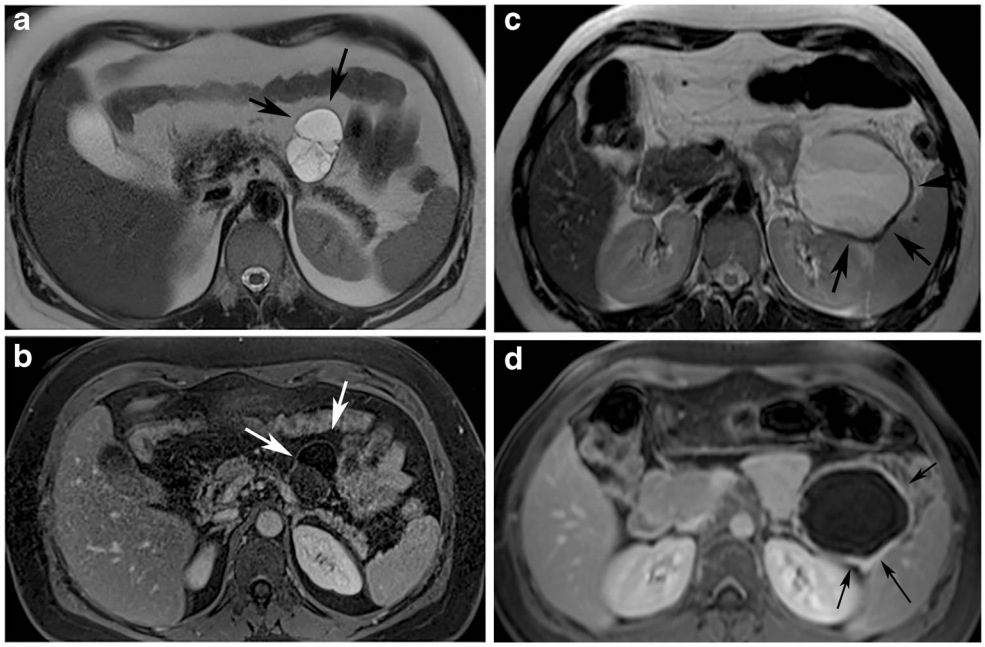


Fig. 4 Cystic neoplasms arising in the body/tail of the pancreas: presence of peripheral wall. **a** Axial T2-weighted half Fourier single-shot turbo spin-echo (HASTE) (TR/TE ∞/90 ms) image shows a cystic neoplasms of the body/tail of the pancreas with oligocystic pattern and without peripheral wall (*arrows*), representing an SCA at histopathology. **b** The peripheral wall shows no significant enhancement on post gadolinium chelate injection, fat-suppressed, volumetric T1-weighted gradient echo image (VIBE) (TR/TE 4.66/1.87 ms) during the portal phase (*arrows*). **c** Axial T2-weighted turbo spin echo (TSE) (TR/TE 4,200/102 ms) image shows a cystic neoplasm of the body/tail of the pancreas with unicystic pattern and a hypointense peripheral wall (*arrows*) that shows contrast enhancement on post-contrast fat-suppressed, volumetric T1-weighted gradient echo image (VIBE) (TR/TE 4.66/1.87 ms) during the portal phase (**d**). Peripheral wall was observed in 88.5 % of MCNs and 11.5 % of SCAs (p<000.1)

2/27 (7 %) of the lesions (Figs. 1 and 2). Regarding the number of cysts observed within the neoplasms, SCAs showed an oligocystic (≤5 cysts) pattern in 12/27 (44 %), multicystic (>6 cysts) in 11/27 (41 %) and unicystic pattern in 4/27 lesions (Figs. 1 and 2).

Lesion margins appeared sharp in 27/27 SCAs observed in ours series.

On T1-WI, SCAs appeared hypointense in 23/27 (85 %) of the cases, isointense relative to the liver in 3/27 (11 %) lesions and hyperintense in 1/27 (4 %) of the lesions. On T2-WI, SCAs appeared hyperintense in 27/27 of the cases (Figs. 1 and 2).

A central scar was observed in 8/27 (30 %) SCAs observed in the body/tail of the pancreas (Fig. 4).

Contrast enhancement of internal septae in 18/27 (67 %) SCAs, whereas contrast enhancement of the peripheral wall and mural nodules was observed respectively in 3/27 (11 %) and 1/27 (4 %) SCAs.

The upstream MPD appeared dilated with a tortuous path in 9/27 (33 %) SCAs (Fig. 6), whereas in 18/27 (67 %) the upstream MPD appeared non-dilated with a linear path. Endoluminal filling defects within the lumen of the MPD were observed in 1/27 (4 %) SCAs, and dilated side branches in the upstream pancreatic duct system were observed in 4/27 (15 %) SCAs.

Hypointensity of the upstream pancreatic parenchyma was observed in none of the SCAs arising in the body/tail of the pancreas.

The comparison of the qualitative image analysis parameters between SCAs and MCNs, as observed on MRI/MRCP images, is reported in Table 3.

Quantitative image analysis

The overall median maximum diameter of cystic neoplasms occurring in the body/tail of the pancreas was 40.0 mm (range 9–118 mm). The overall median peripheral wall thickness was 2.8 mm (range 1–7 mm). The median upstream calibre of the main pancreatic duct was 1.5 mm (range 1–3 mm).

The median maximum diameter of MCNs was 54.0 mm (range 16–118 mm). The median peripheral wall thickness of MCNs was 4.0 mm (range 1–7 mm). The median upstream calibre of the main pancreatic duct was 1.5 mm (range 1–3 mm).

The median maximum diameter of SCAs was 32.0 mm (range 9–92 mm). The median peripheral wall thickness of SCAs was 2.0 mm (range 1–4 mm). The median upstream calibre of the main pancreatic duct was 1.6 mm (range 1–3 mm).

The comparison of the quantitative parameters, as observed on MRI/MRCP images, of SCAs and MCNs is reported in Table 4.

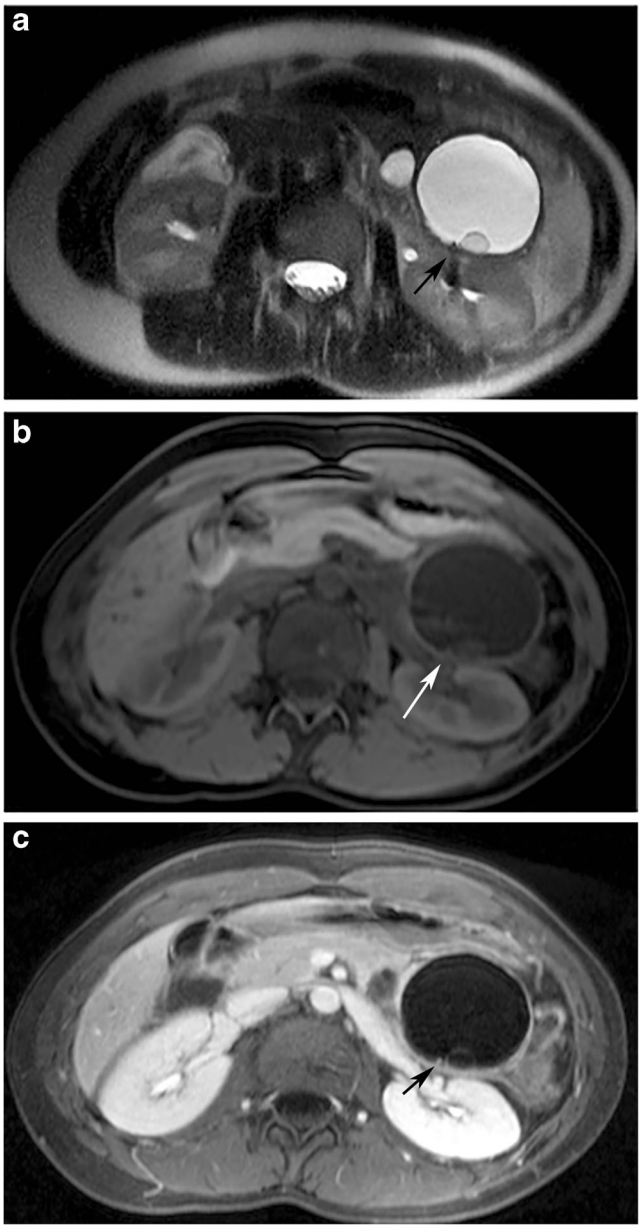


Fig. 5 Cystic neoplasms arising in the body/tail of the pancreas: central scar: mural nodules. **a** Axial T2-weighted half Fourier single-shot turbo spin-echo (HASTE) (TR/TE ∞/90 ms) image shows a cystic neoplasms of the body/tail of the pancreas with oligocystic pattern, peripheral wall and a mural nodule (*arrow*). The mural nodule does show flow void on non-contrast fat-suppressed, volumetric T1-weighted gradient echo image (VIBE) (TR/TE 4.66/1.87 ms) (*arrow* in **b**), and displays contrast enhancement on post-contrast fat-suppressed, volumetric T1-weighted gradient echo image (VIBE) (TR/TE 4.66/1.87 ms) during the portal phase (*arrow* in **c**)

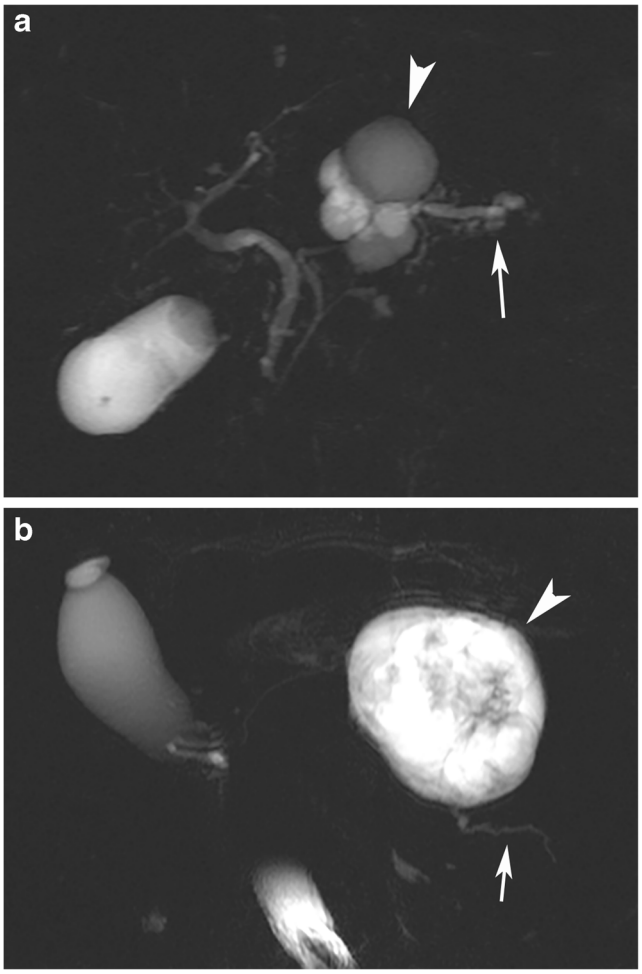


Fig. 6 Cystic neoplasms arising in the body/tail of the pancreas: compression of the main pancreatic duct (MPD). **a** Coronal and axial **b** T2-weighted magnetic resonance cholangiopancreatography (MRCP) images using a fat-suppressed T2-weighted half Fourier single-shot turbo spin-echo (HASTE) (TR/TE ∞/1,100 ms) sequence show a cystic neoplasm in the body/tail of the pancreas (*arrowhead*), responsible for upstream dilatation of the main pancreatic duct (MPD), with tortuous path, and dilation of the side branches, indicative of obstructive chronic pancreatitis (*arrow*), both in SCA (**a**) and MCN (**b**)

Discussion

There is a medical need in cystic pancreatic neoplasms, arising in the body/tail of the pancreas, to identify signs on MR/MRCP imaging helpful for the differential diagnosis between MCNs, candidates for surgery, and SCAs, candidates for clinical and radiological follow-up.

MR imaging is potentially able to cover this medical need because it is able to depict internal structure of pancreatic cystic neoplasms, such as septa and cysts contents, and the neoplasm–ductal system relationship [1, 19–22], by means of MRCP.

MCN, similarly to SCA, lacks communication with the ductal system [23]; however MCNs arise almost exclusively in the body/tail of the pancreas of middle-age women, whereas SCAs arise everywhere in the pancreatic gland [1, 22].

In our series some MR/MRCP imaging features had a statistically different frequency between MCNs and SCAs, and so may be helpful in the differential diagnosis. With

Table 3 Qualitative image analysis of cystic lesions arising in the body/tail of the pancreas: comparison between mucinous cystic neoplasms (MCNs) and serous cystadenomas (SCAs)

		MCNs		SCAs		Total	*p* value
		n=26	%	*n*=27	%		
Macroscopic pattern	<2 cm	2	11.8	15	88.2	17	<0.0001
	Mixed	5	33.3	10	66.7	15	
	≥2 cm	19	90.5	2	9.5	21	
Number of cysts	1	10	71.4	4	28.6	14	0.054
	≤5	12	50.0	12	50.0	24	
	≥6	4	26.7	11	73.3	15	
Lesion margins	Sharp	23	46.0	27	54.0	50	0.069
	Irregular	3	100.0	0	0.0	3	
SI T1-WI	Hypointense	19	45.2	23	54.8	42	0.339
	Isointense	3	50.0	3	50.0	6	
	Hyperintense	4	80.0	1	20.0	5	
SI T2-WI	Hypointense	0		0		0	–
	Isointense	0		0		0	
	Hyperintense	26	49.1	27	50.9	53	
Central scar	Present	0	0	8	29.6	8	0.003
	Absent	26	100	19	70.4	45	
Enhancement intralesional septae	Absent	16	64.0	9	36.0	25	0.04
	Present	10	35.7	18	64.3	28	
Enhancement peripheral wall	Absent	3	11.1	24	88.9	27	<0.0001
	Present	23	88.5	3	11.5	26	
Enhancement mural nodules	Absent	10	27.8	26	72.2	36	<0.0001
	Present	16	94.1	1	5.9	17	
Upstream MPD	Linear	21	53.8	18	46.2	39	0.244
	Tortuous	5	35.7	9	64.3	14	
Endoluminal filling defects	Absent	24	48.0	26	52.0	50	0.53
	Present	2	66.7	1	33.3	3	
Upstream dilated side branches	Absent	23	50.0	23	50.0	46	0.725
	Present	3	42.9	4	57.1	7	
Hypointensity of upstream pancreatic parenchyma on T1-WI	Absent	21	43.8	27	56.3	48	0.017
	Present	5	100	0	0	0	

MCNs mucinous cystic neoplasms, *SCAs* serous cystadenomas, *SI T1-WI* signal intensity on T1-weighted images, *SI T2-WI* signal intensity on T2-weighted images, *MPD* main pancreatic duct

regard to the macroscopic pattern of the cystic neoplasms, MR/MRCP imaging of MCNs showed a macrocystic pattern in 90.5 % (19/26) of the cases, whereas SCAs showed a microcystic pattern in 88.2 % (15/27) of the cystic neoplasms ($p<0.0001$). The presence of a central scar is also another helpful sign for the differential diagnosis between SCAs and MCNs: in our series this was observed in 29.6 % (8/27) of SCAs and none of the MCNs ($p=0.003$).

Table 4 Quantitative image analysis of cystic lesions arising in the body/tail of the pancreas: comparison between mucinous cystic neoplasms (MCNs) and serous cystadenomas (SCAs)

	MCNs *n*=26		SCAs *n*=27		
	mm	IQR	mm	IQR	*p* value
Median maximum diameter of the cysts	54	40; 73	32	20; 44	0.001
Median wall thickness	4	2; 4	2	2; 3	<0.0001
Median upstream MPD calibre	2	1; 2	2	1; 2	0.215

MCNs mucinous cystic neoplasms, *SCAs* serous cystadenomas, *IQR* interquartile range

Other findings detected in our series could be helpful in the differential diagnosis between MCNs and SCAs: namely the thickness of the peripheral wall of the neoplasm and its enhancement during the portal venous/equilibrium phase of the dynamic study following intravenous administration of gadolinium chelates. In fact, the median wall thickness of MCNs of our series was significantly larger compared to SCAs ($p<0.0001$). This finding is in agreement with the theory expressed by Zamboni et al. [4], stating that between the fourth and sixth week of gestation during the

embryological stage, primordial ovarian cells could be incorporated within the pancreatic parenchyma owing to the proximity of the left primordial gonad and the dorsal pancreatic anlage. The primordial ovarian cells are most likely circumscribed by the parenchyma of the dorsal pancreatic anlage, and this process may be the cause of a subsequent development of a peripheral wall. According to this development, at histopathology, cystic walls and septae of MCNs are lined by mucin-producing epithelium supported by a distinctive ovarian-type stroma. Stromal cells are positive for progesterone and oestrogen receptors in 48 % and 22 % of the cases respectively [5].

MCNs vary in size from a few millimetres to 35 cm [4–6] and have malignant potential. The incidence of carcinoma in situ increases with the size and the complexity of the lesion. In the current study the diagnostic imaging suggestive of dysplasia/malignancy is represented by the presence of mural nodules, which were depicted in 94.1 % (16/26) of the patients with MCN and 5.9 % (1/27) of the patients with SCA ($p<0.0001$). However mural nodule occurred both in non-invasive (16/16) and invasive (1/17) MCNs; therefore this is suggestive of dysplasia instead of invasiveness.

MCNs and SCAs are equally responsible for a compression on the main pancreatic duct with upstream signs of chronic pancreatitis ($p=0.725$). This suggests that the mass effect exerted on adjacent structures by the cystic neoplasm is independent from the type of neoplasm and from its biological behaviour.

To overcome diagnostic imaging limitations genetic anomalies, detected on the intralesional fluid analysis, have been recently suggested to distinguish the harmless SCAs from the low-grade malignant MCNs that have the capacity to progress to cancer. The combination of molecular analysis with clinical and radiological data may lead to more accurate diagnosis [25].

In clinical practice a differential diagnosis should always be made to distinguish MCNs from other neoplastic (intraductal papillary mucinous neoplasms (IPMNs), cystic neuroendocrine tumours) and non-neoplastic lesions (pseudocysts).

At diagnostic imaging for instance, MCNs can be differentiated from IMPNs by depicting the connection with the pancreatic duct system by means of MR/MRCP images [22]; this is lacking in MCNs and present in IPMNs. However, in some cases neuroendocrine tumours (NETs) of the pancreas may have characteristics of cystic lesions with a thick wall, which presents enhancement during the arterial-portal phase of the dynamic study [24]; so it may be difficult to distinguish between MCNs and cystic NETs.

Unfortunately, there is also a significant overlap between the imaging appearances of cystic neoplasms and pseudocysts [22]; therefore in every patient it is important to investigate for previous episodes of pancreatitis.

Our study has limitations mainly related to the retrospective nature of the study and to the small number of cases, as a result of the rarity of these tumours. We retrospectively included in the study patients with known diagnosis of MCNs and SCAs, and we excluded patients with IPMNs. This decision is based on the presence/lack of communication with the pancreatic duct systems that is the criterion to differentiate IPMNs from other cystic neoplasms of the pancreas. However, in clinical practice this differentiation may sometimes not be so easy.

Non-communicating cystic neoplasms arising in the body/tail of the pancreas may encompass MCNs and SCAs that show a different biological behaviour and consequently a different treatment, namely surgery for MCNs and follow-up for SCAs. MR imaging is the diagnostic imaging procedure most suitable for this differential diagnosis, because of its high contrast resolution and its capability of simultaneously assessing the pancreatic duct system and pancreatic parenchyma. In our series the MR imaging criteria useful for the differential diagnosis between MCNs and SCAs, arising in the body/tail of the pancreas, are the macroscopic pattern: macrocystic for MCNs and microcystic for SCAs; the presence of a central scar suggestive of SCA; and the presence of a measurable peripheral wall and mural nodules suggestive of MCNs.

Acknowledgements The scientific guarantor of this publication is Roberto Pozzi Mucelli. The authors of this manuscript declare no relationships with any companies whose products or services may be related to the subject matter of the article. The authors state that this work has not received any funding. One of the authors has significant statistical expertise. Institutional review board approval was obtained. Written informed consent was waived by the institutional review board. Methodology: retrospective, observational, performed at one institution.

References

1. Basturk O, Coban I, Adsay NV (2009) Pancreatic cysts: pathologic classification, differential diagnosis, and clinical implications. Arch Pathol Lab Med 133:423–438
2. Compagno J, Oertel JE (1978) Mucinous cystic neoplasms of the pancreas with overt and latent malignancy (cystadenocarcinoma and cystadenoma). A clinicopathologic study of 41 cases. Am J Clin Pathol 69:573–580
3. Tanaka M, Chari S, Adsay V et al (2006) International consensus guidelines for management of intraductal papillary mucinous neoplasms and mucinous cystic neoplasms of the pancreas. Pancreatology 6:17–32
4. Zamboni G, Fukushima N, Hruban R, Klöppel G (2010) Mucinous cystic neoplasms of the pancreas. In: Bosman FT, Carneiro F, Hruban RH, Theise ND (eds) WHO classification of tumours of the digestive system. IARC, Lyon, pp 300–303
5. Zamboni G, Scarpa A, Bogina G et al (1999) Mucinous cystic tumors of the pancreas: clinicopathological features, prognosis, and relationship to other mucinous cystic tumors. Am J Surg Pathol 23:410–422
6. Thompson LD, Becker RC, Przygodzki RM, Adair CF, Heffess CS (1999) Mucinous cystic neoplasm (mucinous cystadenocarcinoma of

low-grade malignant potential) of the pancreas: a clinicopathologic study of 130 cases. Am J Surg Pathol 23:1–16
7. Crippa S, Salvia R, Warshaw AL et al (2008) Mucinous cystic neoplasm of the pancreas is not an aggressive entity: lessons from 163 resected patients. Ann Surg 247:571–579
8. Fritz S, Warshaw AL, Thayer SP (2009) Management of mucin-producing cystic neoplasms of the pancreas. Oncologist 14:125–136
9. Gaujoux S, Brennan MF, Gonen M et al (2011) Cystic lesions of the pancreas: changes in the presentation and management of 1,424 patients at a single institution over a 15-year time period. J Am Coll Surg 212:590–600, discussion 600–593
10. Bassi C, Salvia R, Molinari E, Biasutti C, Falconi M, Pederzoli P (2003) Management of 100 consecutive cases of pancreatic serous cystadenoma: wait for symptoms and see at imaging or vice versa? World J Surg 27:319–323
11. Manfredi R, Bonatti M, D'Onofrio M et al (2012) Incidentally discovered benign pancreatic cystic neoplasms not communicating with the ductal system: MR/MRCP imaging appearance and evolution. Radiol Med. doi:10.1007/s11547-012-0837-3
12. Crippa S, Fernandez-Del Castillo C, Salvia R et al (2010) Mucin-producing neoplasms of the pancreas: an analysis of distinguishing clinical and epidemiologic characteristics. Clin Gastroenterol Hepatol 8:213–219
13. Manfredi R, Graziani R, Motton M et al (2009) Main pancreatic duct intraductal papillary mucinous neoplasms: accuracy of MR imaging in differentiation between benign and malignant tumors compared with histopathologic analysis. Radiology 253:106–115
14. Sahani DV, Kadavigere R, Saokar A, Fernandez-del Castillo C, Brugge WR, Hahn PF (2005) Cystic pancreatic lesions: a simple imaging-based classification system for guiding management. Radiographics 25:1471–1484
15. Salvia R, Partelli S, Crippa S et al (2009) Intraductal papillary mucinous neoplasms of the pancreas with multifocal involvement of branch ducts. Am J Surg 198:709–714
16. Berland LL, Silverman SG, Gore RM et al (2010) Managing incidental findings on abdominal CT: white paper of the ACR incidental findings committee. J Am Coll Radiol 7:754–773
17. Lee KS, Sekhar A, Rofsky NM, Pedrosa I (2010) Prevalence of incidental pancreatic cysts in the adult population on MR imaging. Am J Gastroenterol 105:2079–2084
18. Kalb B, Sarmiento JM, Kooby DA, Adsay NV, Martin DR (2009) MR imaging of cystic lesions of the pancreas. Radiographics 29: 1749–1765
19. Reddy RP, Smyrk TC, Zapiach M et al (2004) Pancreatic mucinous cystic neoplasm defined by ovarian stroma: demographics, clinical features, and prevalence of cancer. Clin Gastroenterol Hepatol 2: 1026–1031
20. Andrejevic-Blant S, Kosmahl M, Sipos B, Kloppel G (2007) Pancreatic intraductal papillary-mucinous neoplasms: a new and evolving entity. Virchows Arch 451:863–869
21. Kosmahl M, Pauser U, Peters K et al (2004) Cystic neoplasms of the pancreas and tumor-like lesions with cystic features: a review of 418 cases and a classification proposal. Virchows Arch 445:168–178
22. Griffin N, Charles-Edwards G, Grant LA (2012) Magnetic resonance cholangiopancreatography: the ABC of MRCP. Insights Imaging 3: 11–21
23. Delavaud C, d'Assignies G, Cros J et al (2014) CT and MR imaging of multilocular acinar cell cystadenoma: comparison with branch duct intraductal papillary mucinous neoplasia (IPMNs). Eur Radiol. doi:10.1007/s00330-014-3248-0
24. Manfredi R, Bonatti M, Mantovani W et al (2013) Non-hyperfunctioning neuroendocrine tumours of the pancreas: MR imaging appearance and correlation with their biological behaviour. Eur Radiol 23:3029–3039
25. Wu J, Jiao Y, Dal Molin M et al (2011) Whole-exome sequencing of neoplastic cysts of the pancreas reveals recurrent mutations in components of ubiquitin-dependent pathways. Proc Natl Acad Sci U S A 108:21188–21193